Published OnlineFirst October 6, 2009; DOI: 10.1158/0008-5472.CAN-08-4889

Inhibition of Tumor Cell Growth, Invasion, and Metastasis by EXEL-2880 (XL880, GSK1363089), a Novel Inhibitor of HGF and VEGF Receptor Tyrosine Kinases

Fawn Qian,[1] Stefan Engst,[1] Kyoko Yamaguchi,[1] Peiwen Yu,[1] Kwang-Ai Won,[1] Lillian Mock,[1] Tracy Lou,[1] Jenny Tan,[1] Connie Li,[1] Danny Tam,[1] Julie Lougheed,[1] F. Michael Yakes,[1] Frauke Bentzien,[1] Wei Xu,[1] Tal Zaks,[2] Richard Wooster,[2] Joel Greshock,[2] and Alison H. Joly[1]

[1]Exelixis, Inc., South San Francisco, California and [2]GlaxoSmithKline R&D, Division of Oncology, Collegeville, Pennsylvania

Abstract

The Met receptor tyrosine kinase and its ligand, hepatocyte growth factor (HGF), are overexpressed and/or activated in a wide variety of human malignancies. Vascular endothelial growth factor (VEGF) receptors are expressed on the surface of vascular endothelial cells and cooperate with Met to induce tumor invasion and vascularization. EXEL-2880 (XL880, GSK1363089) is a small-molecule kinase inhibitor that targets members of the HGF and VEGF receptor tyrosine kinase families, with additional inhibitory activity toward KIT, Flt-3, platelet-derived growth factor receptor β, and Tie-2. Binding of EXEL-2880 to Met and VEGF receptor 2 (KDR) is characterized by a very slow off-rate, consistent with X-ray crystallographic data showing that the inhibitor is deeply bound in the Met kinase active site cleft. EXEL-2880 inhibits cellular HGF-induced Met phosphorylation and VEGF-induced extracellular signal-regulated kinase phosphorylation and prevents both HGF-induced responses of tumor cells and HGF/VEGF-induced responses of endothelial cells. In addition, EXEL-2880 prevents anchorage-independent proliferation of tumor cells under both normoxic and hypoxic conditions. *In vivo*, these effects produce significant dose-dependent inhibition of tumor burden in an experimental model of lung metastasis. Collectively, these data indicate that EXEL-2880 may prevent tumor growth through a direct effect on tumor cell proliferation and by inhibition of invasion and angiogenesis mediated by HGF and VEGF receptors. [Cancer Res 2009;69(20):8009–16]

Introduction

Met is a receptor tyrosine kinase (RTK) that is widely expressed in epithelial and endothelial cells, whereas its ligand, hepatocyte growth factor (HGF), is expressed by cells of the mesenchymal lineage (1). Met is a central mediator of cell growth, survival, motility, and morphogenesis during development; however, its role in adults appears to be primarily confined to repair/regeneration following injury of tissues such as the liver (2). Overexpression of Met has been widely documented in many human tumor types (1, 3) and activating Met mutations have been identified in hereditary and sporadic papillary renal cell carcinoma (4, 5), in gastric (6), hepatocellular (7), head and neck (8), and ovarian (9) carcinomas, and in other tumor types including small cell lung cancer (10), breast cancer (11), and glioma (12). Notably, Met mutations appear to be particularly prevalent in metastatic lesions, consistent with a role for Met in promoting tumor invasion and dissemination (8, 13). Met gene amplification has been found in gastric and colorectal tumors (14–17) and was recently proposed as a mechanism for acquired resistance to epidermal growth factor receptor inhibitors in lung cancer (18, 19). Clinically, overexpression and/or dysregulation of Met and/or HGF correlates with a poor prognostic outcome in patients with a diverse array of malignancies (20–24).

The negative prognostic consequences of Met dysregulation in tumors reflect its multiple roles in tumor pathobiology (reviewed in refs. 1, 3). Activated Met promotes cancer cell growth and survival and increases their motility and invasiveness, facilitating tumor metastasis. In addition, activation of Met in endothelial cells by HGF promotes tumor angiogenesis. Dysregulation of Met signaling results in enhanced tumorigenicity and metastatic potential in engineered cells and in transgenic mice (25–28). Conversely, inhibition of Met signaling using ribozymes, antisense RNA, anti-HGF antibodies, or an inhibitory fragment of HGF inhibits growth of tumor xenografts in mice (29–35).

The receptors for vascular endothelial growth factor (VEGF), VEGF receptor 1 and VEGF receptor 2/KDR, are expressed on the surface of vascular endothelial cells and on some bone marrow–derived cells (36). When activated, these receptors mediate endothelial cell invasion, proliferation, and survival. VEGF expression is up-regulated in many human tumors, and activation of KDR by VEGF is believed to be a major driver of tumor angiogenesis. Consistent with this, inhibition of VEGF signaling in preclinical models inhibits tumor angiogenesis and tumor growth (36, 37). The anti-VEGF monoclonal antibody bevacizumab (Avastin) has shown therapeutic benefit in patients, and many other antiangiogenic agents are undergoing clinical trials.

In addition to their individual roles in tumor pathobiology, Met and KDR cooperate to promote tumor angiogenesis. Expression of Met is regulated by the same hypoxia-inducible factor system that governs VEGF expression levels; hence, both Met and VEGF are induced in response to tumor hypoxia (38). This may explain the observation that the presence of tumor hypoxia is a negative prognostic indicator for tumor dissemination and patient prognosis (39). There is also evidence for cooperativity between Met and KDR in endothelial cells: simultaneous administration of HGF and VEGF in cultured primary endothelial cells confers a greater proliferative stimulus and proangiogenic effect than either ligand alone (40).

Note: Supplementary data for this article are available at Cancer Research Online (http://cancerres.aacrjournals.org/).

Requests for reprints: Alison H. Joly, Exelixis, Inc., 170 Harbor Way, South San Francisco, CA 94083. Phone: 650-837-7000; Fax: 650-837-8315; E-mail: ajoly@exelixis.com.

doi:10.1158/0008-5472.CAN-08-4889

Published OnlineFirst October 6, 2009; DOI: 10.1158/0008-5472.CAN-08-4889

These findings suggest that simultaneous inhibition of Met and KDR by a small-molecule inhibitor may confer broad and potent antitumor efficacy.

We report here the characterization of EXEL-2880, an inhibitor of the HGF and VEGF RTK families. EXEL-2880 binds tightly to Met and KDR with a very slow off-rate, consistent with the mode of binding revealed by X-ray crystallography. EXEL-2880 inhibits cellular HGF-induced Met phosphorylation and VEGF-induced extracellular signal-regulated kinase phosphorylation and inhibits growth of tumor cells under both normoxic and hypoxic conditions with increased potency against Met-amplified gastric cancer cell lines. *In vitro*, EXEL-2880 inhibits HGF-induced responses of tumor cells and HGF/VEGF-induced responses of endothelial cells that are thought to contribute to invasion, metastasis, and angiogenesis *in vivo*. Consistent with this profile, EXEL-2880 inhibits tumor formation in an *in vivo* murine model of lung metastasis. EXEL-2880 therefore has the potential to prevent tumor growth through a direct effect on tumor cell proliferation and indirectly through inhibition of the host angiogenic response.

Materials and Methods

Compound. EXEL-2880 (Supplementary Fig. S1) was synthesized at Exelixis (41) and its synthesis will be reported separately. The compound was licensed to GSK in December 2007 and is now called GSK1363089.

Kinase inhibition assays. Kinase inhibition was investigated using one of three assay formats: [^{33}P]phosphoryl transfer, luciferase-coupled chemiluminescence, or AlphaScreen tyrosine kinase technology (Perkin-Elmer). Further assay details are provided in Supplementary Section. IC_{50} values were calculated by nonlinear regression analysis using XLFit.

Expression and X-ray crystallography of Met receptor. The Met kinase domain (1051-1348) was expressed with a NH_2-terminal histidine tag and Tobacco Etch Virus protease cleavage site (MLLGSHHHHHHGENLYFQGS) in Sf9 insect cells using a modified pAcGP67 baculovirus DNA transfer vector (BD Pharmingen). Further details of protein purification and X-ray crystallography are provided in Supplementary Section.

Cell lines, cell culture conditions, and cytotoxic screening. Cell lines B16F10, PC-3, A549, HT29, and MDA-MB-231 were purchased from the American Type Culture Collection and propagated using recommended conditions. Human umbilical vein endothelial cells, human lung microvascular endothelial cells (HMVEC-L), and normal human dermal fibroblasts were obtained from Clonetics and propagated according to the manufacturer's instructions. For cytotoxic screening, a panel of 91 cancer cell lines was purchased (American Type Culture Collection; Developmental Therapeutics Program, National Cancer Institute; German Collection of Microorganisms and Cell Cultures; and European Collection of Cell Cultures) and maintained according to the supplier's specifications or RPMI 1640 supplemented with 10% fetal bovine serum (FBS), 2 mmol/L Glutamax, and 1 mmol/L sodium pyruvate. Microarray analysis was done as described in Supplementary Data. These data are available at https://cabig.nci.nih.gov/caArray_GSKdata/.

Target receptor phosphorylation assays. PC-3 and B16F10 cells were seeded in 24-well plates overnight. The cells were then washed and incubated with serum-free medium for 3 h followed by a 1 h incubation with EXEL-2880 before addition of HGF (100 ng/mL; R&D Systems) for 10 min. Met phosphorylation status was determined by ELISA analysis (Supplementary Data). For determination of VEGF-stimulated extracellular signal-regulated kinase phosphorylation, human umbilical vein endothelial cells were seeded in 96-well plates and incubated for 24 h and then serum-starved for another 24 h. A serial dilution of EXEL-2880 was added for 1 h before a 5 min stimulation with VEGF (20 ng/mL; R&D Systems). Medium was removed, and the cells were fixed with Cytofix (BD Pharmingen) and then treated with 0.6% H_2O_2. Plates were blocked with 10% FBS and incubated with a mouse monoclonal anti-phosphorylated extracellular signal-regulated kinase p44/42 antibody (E10; Cell Signaling Technology) followed by incubation with goat anti-mouse IgG-horseradish peroxidase (BD Pharmingen) and chemiluminescent detection. IC_{50} values were calculated based on triplicate experiments.

HGF-induced migration assay. B16F10 cells (2×10^5) were seeded onto 0.8 μm membranes in the top chamber of a 96-well Transwell plate in DMEM containing a serial dilution of EXEL-2880 and 0.1% FBS. DMEM containing HGF (50 ng/mL), 0.2% FBS, and EXEL-2880 was added to the bottom chamber, and after 24 h, the medium was removed and Accutase (ISC BioExpress) was added to the bottom chamber. After 30 min, cells were transferred to a V-bottomed 96-well plate, centrifuged, and resuspended in HBSS containing 2 mg/mL calcein-AM (Molecular Probes). After incubation for 30 min, cells were transferred into a black 96-well plate. Fluorescence emission was measured at 480 nm using an excitation wavelength of 520 nm and imaged with a fluorescence microscope.

HGF-induced invasion assay. Growth factor reduced Matrigel (15 μL; BD Pharmingen) was coated onto 0.8 μm membranes in 96-well Transwell plates (Millipore) and incubated for 30 min. B16F10 cells (1×10^5) were plated in the top chamber in DMEM containing dilutions of EXEL-2880 and 0.1% FBS. HGF (50 ng/mL), 0.2% FBS, and EXEL-2880 were added to the bottom chamber. After 24 h, the medium was removed and the cells visualized as described for the migration assay above.

Soft-agar assay. B16F10, A549, and HT29 cells (1.2×10^3 per well) were mixed with soft agar and seeded in a 96-well plate containing 10% FBS and EXEL-2880 over a base agar layer. For normoxic conditions, the plates were incubated (37°C) for 12 to 14 days in 21% oxygen, 5% CO_2, and 74% nitrogen, whereas incubation (37°C) under hypoxic conditions was done in a hypoxia chamber (IN VIVO2 400; Biotrace) in 1% oxygen, 5% CO_2, and 94% nitrogen. The number of colonies was evaluated under each condition following addition of 50% Alamar Blue (Invitrogen) and fluorescence detection.

Endothelial tubule formation and migration assays. Normal human dermal fibroblasts were plated at 2.5×10^4 per well in 96-well plates and incubated under for 24 h. HMVEC-L cells (6×10^3 per well) were plated onto the normal human dermal fibroblast cultures with 60 ng/mL VEGF or conditioned medium (MDA-MB-231 or B16F10 cells) and EXEL-2880. The cocultures were incubated for 7 days after which cells were fixed with Cytofix (BD Pharmingen) and stained with 2 μg/mL CD31 antibody (clone WM-59; BD Biosciences) followed by anti-mouse IgG-horseradish peroxidase (DAKOCytomation) and AEC color development reagent (DAKOCytomation). Digital images (20×) were taken and total tube length was quantified with Image Pro Plus software (Media Cybernetics). IC_{50} values were calculated based on the average total tubule length achieved in cultures treated with EXEL-2880 compared with cultures treated with VEGF alone. HMVEC-L cells were plated in 96-well plates coated with fibronectin (BD Biosciences), and when confluent, a cell-free zone was introduced into each well using a pipette tip. The cultures were treated with EXEL-2880 in serum-free medium followed by addition of VEGF (30 ng/mL) or HGF (60 ng/mL) in duplicate overnight. The cultures were stained with 0.2 μg/mL calcein-AM (Molecular Probes) for visualization and a quantitative assessment of inhibition of migration was done for each condition.

Cytotoxicity assay. HMVEC-L cells were seeded at 5×10^3 per well in 96-well plates and incubated for 24 h, after which a serial dilution of EXEL-2880 in serum-free medium was added for a further 24 h and cell viability was determined (Alamar Blue; Biosource).

Animals. Female athymic nude mice (NCr or BALB/c) 5 to 8 weeks old were purchased from Taconic. Animals were housed and treated according to the guidelines outlined by the Exelixis Institutional Animal Care and Use Committee.

Pharmacodynamic studies. *In vivo* target modulation studies were done in naive mice or mice bearing B16F10 tumors. EXEL-2880 or vehicle (0.9% normal saline) was administered at 10 mL/kg via oral gavage. For examination of Met phosphorylation in liver, HGF (10 μg/mouse) was administered i.v. 10 min before harvest. For examination of Flk-1/KDR phosphorylation in lung, VEGF (10 μg/mouse) was administered i.v. 30 min before harvest 0.5 h later (42). Receptor phosphorylation analysis was determined by immunoblot analysis.

Efficacy studies. B16F10 tumor cells (2×10^5) were implanted via i.v. tail vein injection into mice on day 0. EXEL-2880 or vehicle administration was

Published OnlineFirst October 6, 2009; DOI: 10.1158/0008-5472.CAN-08-4889

initiated 3 days after implantation for 10 days followed by assessment of lung tumor burden. Lungs were excised, weighed, and zinc-fixed for 24 h, and the number of nodules formed on all lobe surfaces was counted using a Zeiss stereoscope (Carl Zeiss). Lung nodule diameters were morphometrically measured on digitally captured images. Inhibition of tumor burden as measured by lung wet weight was calculated as follows: % tumor growth inhibition = [(compound treated-naive / vehicle-naive) × 100]. The results for each treatment group (n = 10 animals) were averaged, and statistical t test analysis was done comparing each treatment group to the vehicle-treated control.

Results

Inhibition of RTKs. EXEL-2880 inhibits HGF receptor family tyrosine kinases with IC_{50} values of 0.4 nmol/L for Met and 3 nmol/L for Ron. EXEL-2880 also inhibits KDR, Flt-1, and Flt-4 with IC_{50} values of 0.9, 6.8, and 2.8 nmol/L, respectively. In addition, EXEL-2880 inhibits members of the platelet-derived growth factor receptor family and the angiopoietin-1 receptor Tie-2 (Table 1). EXEL-2880 exhibits modest activity against fibroblast growth factor receptor 1 and epidermal growth factor receptor and is inactive against 50 serine/threonine kinases, including cyclin-dependent kinases and protein kinase C isoforms (data not shown).

To determine the mechanism of inhibition by EXEL-2880, IC_{50} determinations for Met and KDR were done in the presence of increasing concentrations of ATP. Figure 1 shows that the IC_{50} values increase linearly with increasing ATP concentration, showing that EXEL-2880 is an ATP-competitive active site inhibitor. The reversibility of enzyme inhibition by EXEL-2880 was also evaluated for Met and KDR. Following 10-fold dilution with 2 mmol/L ATP, ~10% activity for both kinases was observed after 180 min. Measurements beyond this time were not feasible due to instability of the enzyme. K_M^{ATP} values of 2 μmol/L were determined for both Met and KDR using the same assay format. Thus, at 2 mmol/L ATP, >90% recovery of enzyme activity is expected to occur at equilibrium, and from this, a dissociation half life of ~15 h can be estimated. The kinetic constants for EXEL-2880 binding to Met and KDR reveal it to be tightly bound with a long dissociation half-life (Supplementary Table S1).

Structure of EXEL-2880 in complex with Met. Met was cocrystallized with EXEL-2880 and the X-ray crystal structure was solved and refined to a resolution of 2.0 Å (Fig. 2). The structure of the complex shows that EXEL-2880 is well-ordered when bound to Met, occupies the ATP-binding site as well as an adjacent pocket, and makes both important hydrogen bonds and extensive hydrophobic contacts with the protein—many of which are external to the ATP binding pocket. The phenyl malonamide moiety of EXEL-2880 dislodges the phenylalanine of the DFG motif (Phe^{1223}) from its activated conformation ("Phe-in") binding pocket under the C-helix (43). Phe^{1223} then reorients by ~13 Å and forms a stabilized stacking interaction with the central fluorophenyl ring of EXEL-2880. This places the kinase in a pseudo-unactivated conformation where the catalytic machinery has been disrupted ("Phe-out"). On

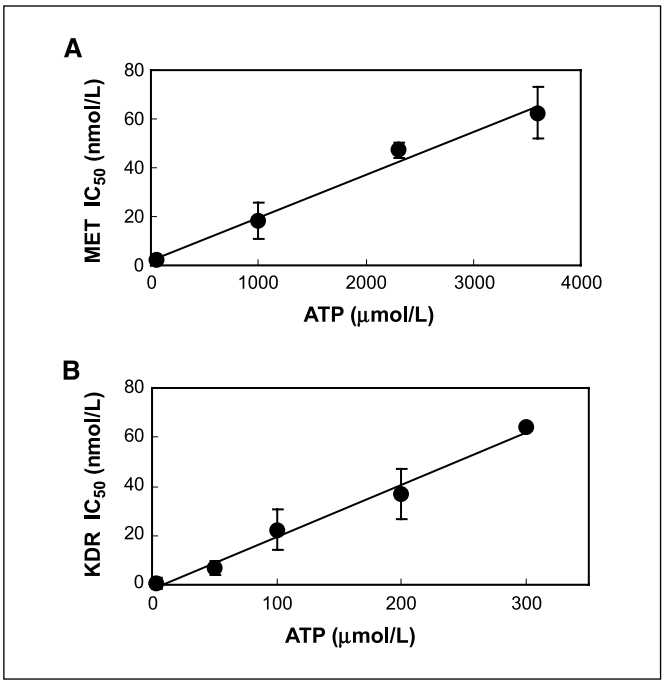

Figure 1. Mechanism of kinase inhibition. *In vitro* kinase assays for Met (*A*) and KDR (*B*) were done using increasing concentrations of ATP. Resulting IC_{50} values were plotted as a function of ATP concentration and shown to exhibit a linear relationship.

Table 1. *In vitro* kinase inhibition profile of EXEL-2880

Kinase	IC_{50} ± SD (nmol/L)	E (nmol/L)	ATP (μmol/L)	Assay
Met	0.4 ± 0.04	0.4	1	C
Ron	3 ± 0.2	3	1	C
KDR	0.86 ± 0.04	0.15	3	C
Flt-1	6.8 ± 0.7	0.13	5	A
Flt-4	2.8 ± 0.4	1	3	A
KIT	6.7 ± 0.6	1	3	A
Flt-3	3.6 ± 0.4	0.5	1	C
Platelet-derived growth factor receptor α	3.6 ± 0.4	0.4	2	C
Platelet-derived growth factor receptor β	9.6 ± 1.1	7	0.5	C
Tie-2	1.1 ± 0.1	1.1	5	R
Fibroblast growth factor receptor 1	660 ± 50	0.1	3	A
Epidermal growth factor receptor	2,990 ± 38	0.2	3	C

NOTE: Mean ± SD of at least three independent determinations.
Assay format abbreviations: A, AlphaScreen; R, radiometric; C, coupled luciferase; E, enzyme concentration assayed.

Published OnlineFirst October 6, 2009; DOI: 10.1158/0008-5472.CAN-08-4889

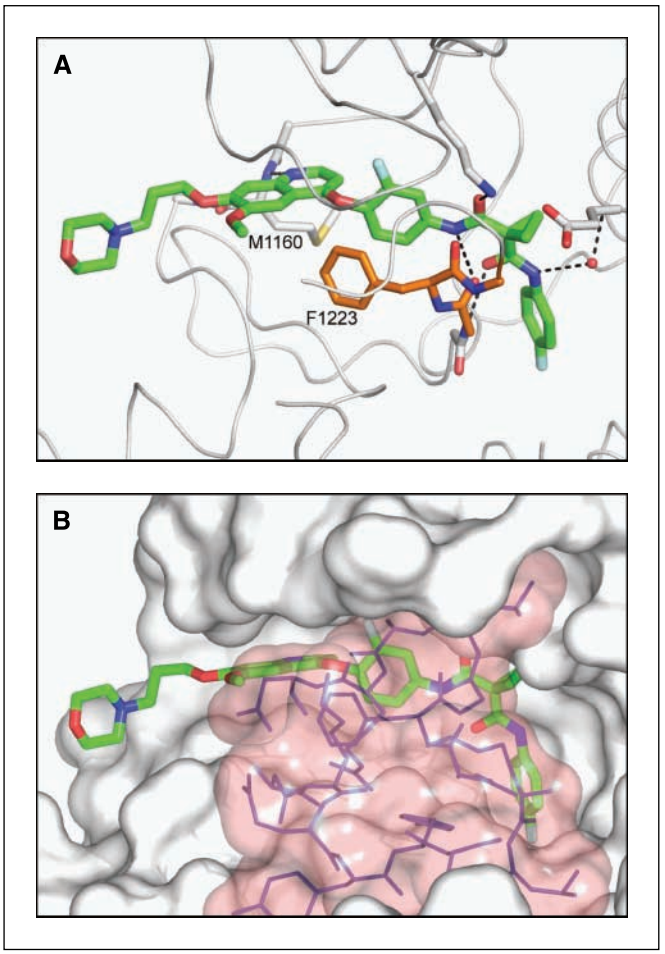

Figure 2. X-ray crystal structure of EXEL-2880 in complex with Met. *A,* EXEL-2880 forms one hydrogen bond with the backbone amide of Met^{1160} in the kinase linker; three additional hydrogen bonds are formed between the malonamide and Met atoms. A water-mediated hydrogen bond is also shown (*water in red*). Phe^{1223} of the activation loop "DFG" (*orange sticks*) has relocated from the position in the active conformation to stack underneath the fluorophenyl ring of the inhibitor, placing the kinase in a pseudo-unactivated conformation. *B,* Met protein surface that forms the binding pocket for EXEL-2880. The activation loop is shown with a transparent surface (*purple sticks*). On binding, a total of 1,225 $Å^2$ of surface area is buried. This is facilitated by the reorganization of the activation loop, which almost entirely buries the ligand, sequestering it from solvent.

binding, a total of 1,225 $Å^2$ of surface area is buried. This is facilitated by the reorganization of the activation loop, which almost entirely buries the ligand, sequestering it from solvent and greatly enhancing the binding affinity.

Inhibition of cellular RTKs. Consistent with the biochemical data described above, EXEL-2880 is a potent inhibitor of cellular Met with IC_{50} values of 23 and 21 nmol/L, respectively, in PC-3 prostate cells and murine B16F10 melanoma cells. To further delineate the cellular effect of EXEL-2880, we used VEGF-induced extracellular signal-regulated kinase phosphorylation to assess the effect of the compound on phosphorylation of KDR in human umbilical vein endothelial cells that resulted in an IC_{50} of 16 nmol/L.

Inhibition of tumor cell migration, invasion, and soft-agar growth. The ability of EXEL-2880 to inhibit HGF-stimulated migration and invasion was tested using *in vitro* assays (44). Murine B16F10 melanoma cells express high levels of Met, which becomes highly phosphorylated when the cells are treated with HGF (Fig. 3*A*). B16F10 cells plated in the top well of a Transwell chamber containing a barrier with 0.8 μm pores show very little ability to migrate to the bottom chamber. Addition of HGF to the bottom chamber greatly increased migration through the barrier over a 24 h period, which was blocked by EXEL-2880 with an IC_{50} value of 44 nmol/L (Fig. 3*C*). Addition of HGF to the bottom chamber again produced a large increase in the number of cells migrating through a Matrigel barrier in response to HGF, and EXEL-2880 inhibited this effect with an IC_{50} value of 25 nmol/L (Fig. 3*D*).

To test the effect of EXEL-2880 on anchorage-independent tumor cell growth, tumor cell suspensions were plated in soft agar and colony formation was monitored for 12 to 14 days. EXEL-2880 inhibited colony growth of B16F10 cells with an IC_{50} value of 40 nmol/L (Fig. 3*B*). Human cell lines A549 and HT29 resulted in IC_{50} values of 29 and 165 nmol/L, respectively (data not shown). Additionally, this experiment was repeated using A549 cells under hypoxic cell culture conditions, which resulted in a colony formation inhibition IC_{50} value of 18 nmol/L.

Inhibition of endothelial tubule formation and migration. When plated on a confluent layer of normal human diploid fibroblast cells, HMVEC-L cells form extensive networks of tubules in response to VEGF (Fig. 4*A*). However, when coincubated with EXEL-2880, VEGF-induced tubule formation was inhibited with an IC_{50} value of 3 nmol/L, which was similar to the IC_{50} value obtained using the VEGF-stimulated extracellular signal-regulated kinase phosphorylation assay described above. As shown in Fig. 4*B*, conditioned medium derived from MDA-MB-231 human breast carcinoma and B16F10 murine melanoma cell cultures stimulated robust tubule formation of HMVEC-L cells (Fig. 4*B*). EXEL-2880 potently inhibited this response to tumor cell–derived growth factors with IC_{50} values of 4 to 5 nmol/L. Additionally, EXEL-2880 showed little cytotoxicity in endothelial cells (IC_{50}, 2,180 nmol/L), indicating that the effects of EXEL-2880 in this cell culture system are clearly antiangiogenic rather than cytotoxic.

A second assay was used to test EXEL-2880 for activity against endothelial cell migration. A cell-free zone was scratched into a monolayer of HMVEC-L cells, and the ability of EXEL-2880 to block VEGF- or HGF-stimulated migration of these cells into the cell-free zone was determined. Figure 4*C* and *D* show that, in the presence of HGF or VEGF, migration of HMVEC-L cells was nearly complete. Moreover, EXEL-2880 reduced migration of HMVEC-L cells in response to HGF and VEGF with IC_{50} values of 17 and 5 nmol/L, respectively.

Cytotoxicity screening panel. To determine the cytotoxic activity of EXEL-2880, a broad panel of cell lines was screened by microarray analysis. These experiments were conducted in the absence of HGF and thus represent activity only where Met is endogenously activated. Overall, the extent of cytotoxic activity generally correlated with high-level expression of known EXEL-2880 targets. Among the most sensitive cell lines, 73% (8 of 11) had extremely high levels of at least one target gene (Supplementary Fig. S2), with gastric tumors exhibiting the highest proportion of sensitive cell lines (50%, 3 of 6). Two of the sensitive gastric cell lines, Hs746T and SNU-5, have both DNA amplification and overexpression of Met. Additional data are available in Supplementary Data.

***In vivo* inhibition of Met and Flk-1/KDR by EXEL-2880.** A single 100 mg/kg oral gavage dose of EXEL-2880 resulted in substantial inhibition of phosphorylation of B16F10 tumor Met, which persisted through 24 h (Fig. 5*A*). In separate experiments, a single oral dose of EXEL-2880 inhibited ligand (e.g., HGF or VEGF)–induced receptor phosphorylation of Met in liver and Flk-1/KDR in lung through 24 h.

Published OnlineFirst October 6, 2009; DOI: 10.1158/0008-5472.CAN-08-4889

The potent and long-lasting pharmacodynamic activity of EXEL-2880 in B16F10 solid tumors prompted efficacy studies in this same model although under different experimental conditions. As shown in Fig. 5*B*, i.v. implantation of B16F10 cells leads to accumulation of tumor cells in the lung where they implant and grow as malignant nodules resembling a model of lung metastasis (45). Once daily oral gavage administration of EXEL-2880 resulted in a dose-dependent reduction in tumor burden of 31% and 62%, respectively, for doses of 30 and 100 mg/kg as determined by a reduction in lung wet weights (Fig. 5*B*). This reduction in lung wet weight was consistent with reductions in both the average size and the number of surface nodules in the lung. The lung surface tumor burden, calculated by multiplying the total nodule count by the average nodule diameter for each tumor, was reduced by 50% and 58% following treatment with 30 and 100 mg/kg EXEL-2880, respectively. In contrast, animals in the vehicle-treated control group exhibited a significant 2-fold increase in lung wet weight compared with animals treated with mock implantation (Supplementary Table S4). In a similar manner, EXEL-2880 treatment of mice bearing B16F10 solid tumors also resulted in dose-dependent tumor growth inhibition of 64% and 87% at 30 and 100 mg/kg, respectively (Supplementary Fig. S3). For both studies, administration of EXEL-2880 was well tolerated with no significant body weight loss.

Discussion

Dysregulation of Met activity has been extensively described in numerous forms of human malignancy and is associated with an aggressive, metastatic phenotype. Multiple point mutations in c-Met have also been documented in tumors including lung, ovarian, and hepatocellular carcinomas. Activating mutations are found in the kinase domain, juxtamembrane domain, and extracellular domain, and mutant forms of c-Met transform cells in culture and promote tumor formation in mice. As documented for other RTKs, many of the point mutations in c-Met found in human tumors are somatic; however, c-Met activating mutations have also been documented in the germ-line. People who inherit activating point mutations in the c-Met kinase domain inevitably develop renal cancer, a syndrome known as hereditary papillary renal cell carcinoma. The pivotal role of VEGF and its receptors in promoting angiogenesis is also well established, and both antibody and small-molecule inhibitors of VEGF signaling have shown utility in the clinic. Rapid up-regulation of both VEGF and Met occurs in tumor cells under hypoxic conditions, and VEGF signaling synergizes with HGF to promote tumor growth, angiogenesis, and invasion. Thus, dual inhibition of Met and VEGF receptors may inhibit growth and survival mechanisms activated by tumor cells in response to hypoxic stress and may be particularly effective in addressing the most lethal aspects of tumor growth, such as migration, invasion, and metastasis. Using this rationale, EXEL-2880 was optimized as a dual inhibitor of Met and KDR RTKs.

Although it was optimized for inhibition of Met and KDR, EXEL-2880 also displays nanomolar potency toward Ron (a close homologue of Met), other VEGF receptors (Flt-1 and Flt-4), c-KIT, platelet-derived growth factor receptors, and Tie-2. This spectrum-selective activity may be advantageous in mediating the antiangiogenic effects of the compound. For example, it has been shown that combined inhibition of both VEGF and platelet-derived growth factor receptors elicits more profound antivascular activity than inhibition of either receptor alone likely due to direct effects on

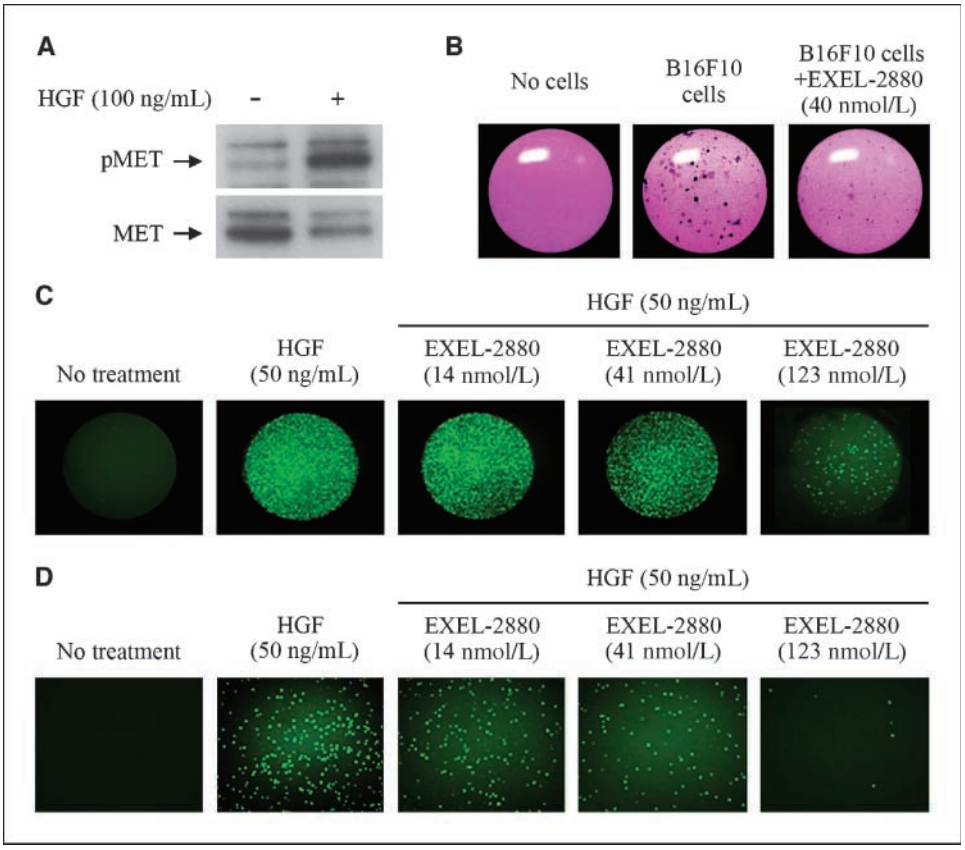

Figure 3. EXEL-2880 inhibits migration, invasion, and anchorage-dependent growth of B16F10 cells. *A,* B16F10 cells were treated with HGF (100 ng/mL) for 10 min, and Met phosphorylation status was determined. *B,* B16F10 cells were plated over a solid layer of soft agar, treated with EXEL-2880 (40 nmol/L), and incubated under normoxic conditions for 12 to 14 d. Quantitation of colony growth relative to nontreated B16F10 cells was done. *C,* B16F10 cells were seeded onto 0.8 μm porous membranes and treated with EXEL-2880 in the presence or absence of HGF (50 ng/mL) for 24 h, and inhibition of migration relative to HGF-alone treated cells was done. *D,* Matrigel was coated onto 0.8 μm porous membranes followed by seeding of B16F10 cells treated with EXEL-2880 in the presence or absence of ligand HGF (50 ng/mL) for 24 h, and the inhibition of invasion relative to HGF alone–treated cells was determined. IC_{50} values were calculated from triplicate experiments. Mean ± SD. Representative images for each treatment group.

Published OnlineFirst October 6, 2009; DOI: 10.1158/0008-5472.CAN-08-4889

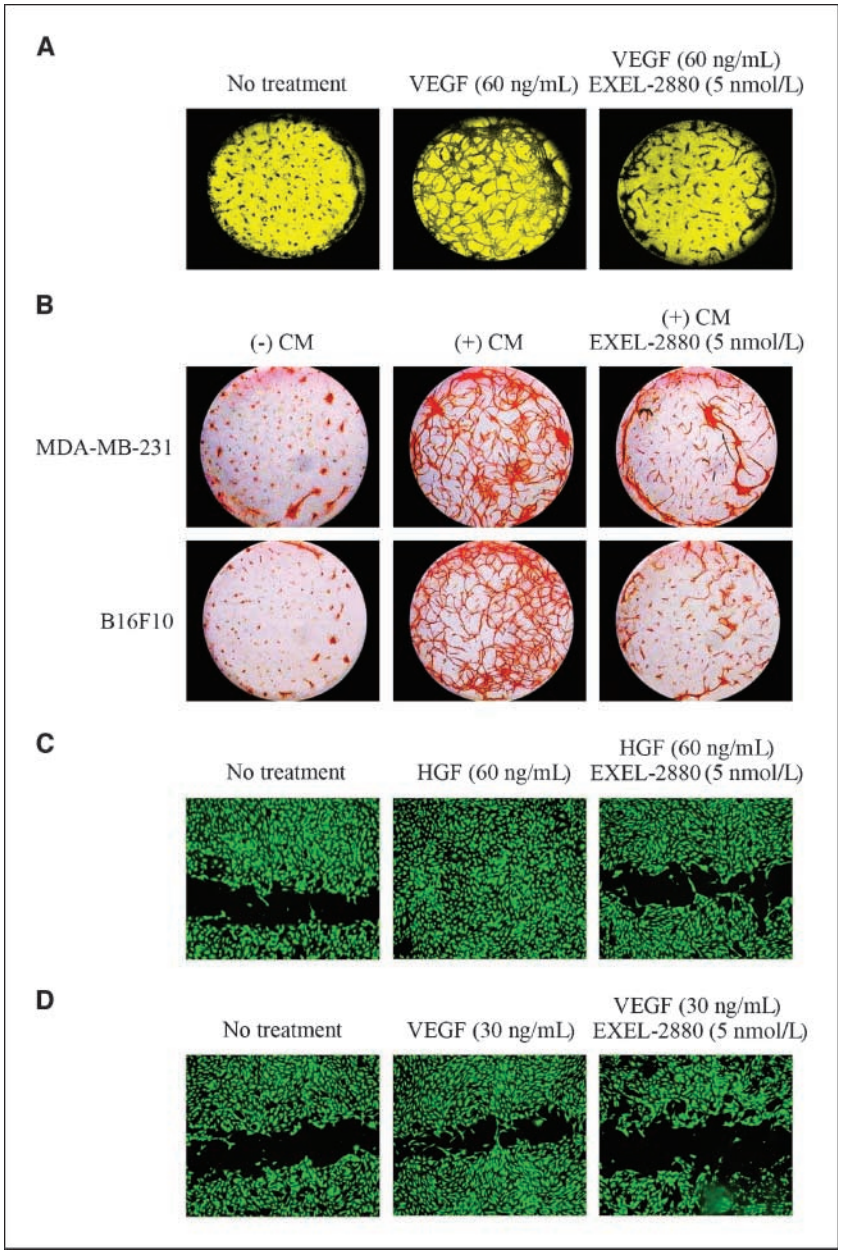

Figure 4. EXEL-2880 inhibits HMVEC-L tubule formation and migration. *A,* HMVEC-L cells cocultured with normal human dermal fibroblasts in the presence of VEGF (60 ng/mL) were treated with EXEL-2880 (5 nmol/L) for 7 d, and inhibition of tubule formation relative to VEGF alone–treated cells was done by immunostaining for CD31. *B,* HMVEC-L cells cocultured with normal human dermal fibroblasts in conditioned MDA-MB-231 or B16F10 medium (*CM*) were treated with EXEL-2880 (5 nmol/L), and inhibition of tubule formation was determined. *C* and *D,* HMVEC-L monolayers were treated with EXEL-2880 (5 nmol/L) in the presence of HGF (60 ng/mL) or VEGF (30 ng/mL), and inhibition of migration was determined. Representative images for each treatment group. IC_{50} values were calculated from triplicate experiments. Mean ± SD.

vascular endothelial cells and indirect effects on the perivascular structure (45).

The binding of EXEL-2880 to both Met and VEGF receptor is characterized by a very slow off-rate *in vitro*. X-ray crystallography revealed that the compound is tightly bound in the active site of Met, with the activation loop burying the compound and sequestering it from solvent. The structure of Met in complex with EXEL-2880 exhibits some unique features compared with the five complexes of Met bound to small-molecule inhibitors (46–48) and two Apo structures (48, 49) that have been reported previously. The inhibitors SU11274, AM7, and K252A all bind to an inactive conformation of Met that closely resembles the Apo unphosphorylated structures, although some differences are observed in the activation loop conformations. In contrast, EXEL-2880 dislodges Phe^{1223} from its binding pocket in the Apo conformation and causes reorganization of the activation loop, such that Phe^{1223} stacks with the fluorophenyl ring of the inhibitor. In contrast to the Apo structure, the C-helix is localized close to the N-lobe, the conserved kinase salt bridge is formed, and the C-helix and salt bridge forms interactions with the inhibitor. Two additional Met inhibitors also have this "Phe-out" conformation for the activation loop as well as a C-helix that is positioned close to the N-lobe, interacting with the bound inhibitor (46). However, in these structures, the conserved salt bridge is not formed; instead, Glu^{1127} forms a hydrogen bond with the inhibitor.

Consistent with its potent and durable inhibition of Met kinase activity *in vitro*, EXEL-2880 is a potent inhibitor of Met phosphorylation in tumor cells and of Met-driven tumor cell responses as evident from the inhibition of both attached and anchorage-independent cell growth and the particularly high sensitivity of c-Met-amplified gastric cancer cell lines. EXEL-2880 also inhibits HGF-driven migration and invasion of B16F10 cells with IC_{50} values similar to those found for receptor phosphorylation. Furthermore, EXEL-2880 inhibits VEGF signaling in endothelial cells and is also a potent inhibitor of endothelial cell migration and tubule formation.

Published OnlineFirst October 6, 2009; DOI: 10.1158/0008-5472.CAN-08-4889

Of note, HMVEC-L migration was inhibited to a similar extent in response to either VEGF or HGF stimulation, consistent with the multitargeted profile of EXEL-2880. EXEL-2880 also blocked *in vitro* endothelial tube formation in response to either VEGF or conditioned medium from tumor cells, suggesting that the array of growth factors secreted by these tumor cells cannot circumvent the antivascular effects of EXEL-2880. Thus, this unique combination of *in vitro* activities, affecting both tumor and endothelial cells, enables a single molecule to reverse three of the six so-called hallmarks of cancer: proliferation, angiogenesis, and invasion/metastasis.

Single-dose oral administration of EXEL-2880 resulted in prolonged inhibition of phosphorylation of constitutively phosphorylated Met in B16F10 solid tumors as well as ligand HGF-stimulated phosphorylation of Met in whole liver. Similar potent activity was observed for inhibition of VEGF-stimulated phosphorylation of Flk-1/KDR in whole lung. This pharmacodynamic activity correlated well with potent efficacy in the B16F10 mouse model of lung metastasis. Oral administration of EXEL-2880 at well-tolerated doses produced a robust, dose-dependent reduction in both the size and the number of lung nodules. In addition, EXEL-2880 treatment resulted in dose-dependent inhibition of B16F10 solid tumors. Collectively, these studies suggest that EXEL-2880 has significant utility in treating primary solid tumors and furthermore may both prevent implantation of metastatic cells and limit the invasive growth of established metastatic lesions, thus affecting perhaps the most lethal phenotype of tumor cells *in vivo*.

Overall, these data show that EXEL-2880 is a highly potent and tight-binding inhibitor of Met and KDR tyrosine kinases and that

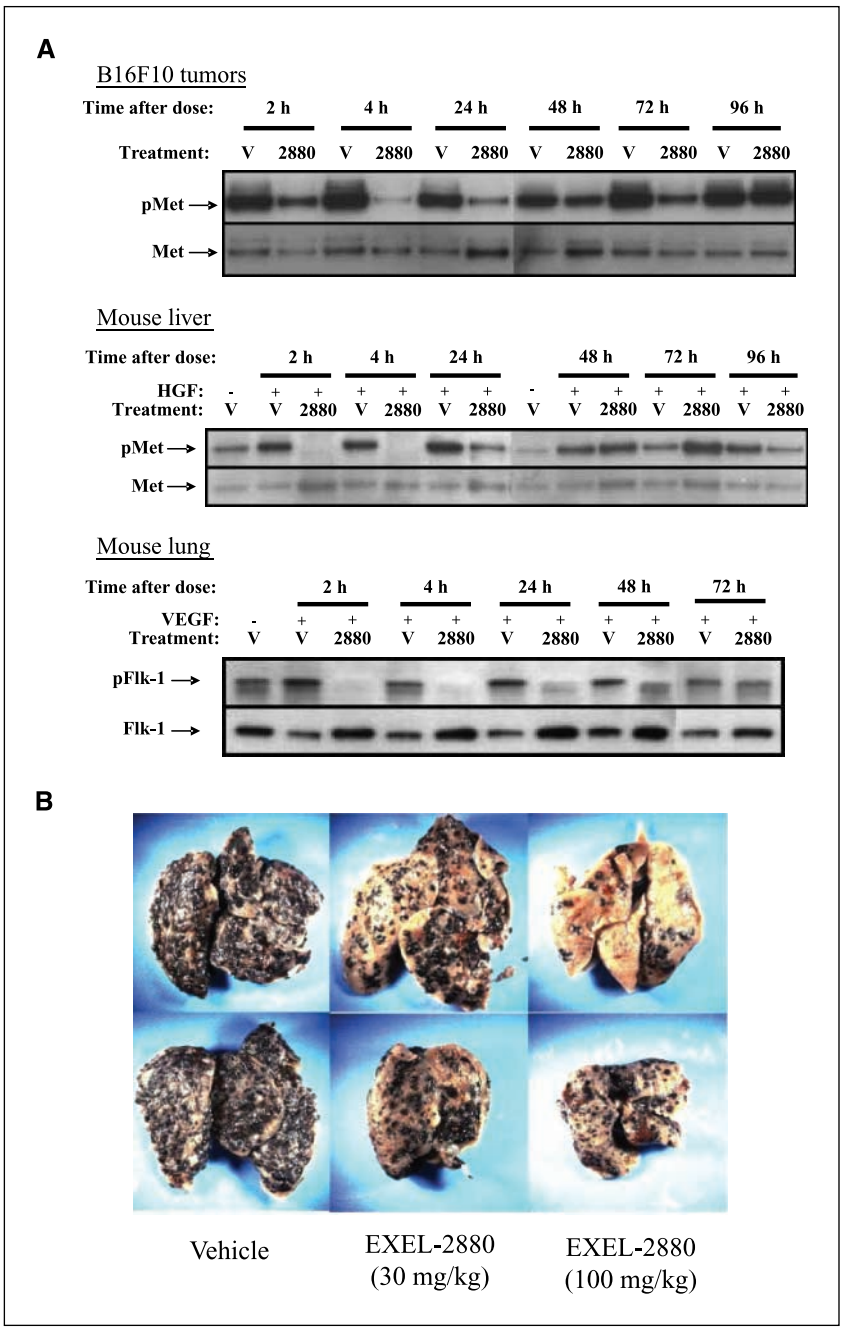

Figure 5. EXEL-2880 inhibits phosphorylation of Met and Flk-1/KDR and reduces tumor burden in an experimental model of lung metastasis. *A,* naive mice or mice bearing B16F10 tumors were administered a single oral gavage dose of EXEL-2880 (100 mg/kg) or vehicle before i.v. administration of HGF (10 μg/mouse) or VEGF (10 μg/mouse). Tissues (tumor, liver, and lung) were collected and lysates were prepared. The relative percent inhibition of phosphorylation of Met and Flk-1/KDR was compared with tissue lysates from vehicle-treated control animals collected at the same time point. *B,* B16F10 cells were implanted into mice via i.v. tail vein injection, and 3 d later, oral gavage administration of EXEL-2880 (30 and 100 mg/kg/d) or vehicle was initiated for 10 d. Lungs were harvested and tumor burden was assessed. Representative images of tumors from each treatment group.

Published OnlineFirst October 6, 2009; DOI: 10.1158/0008-5472.CAN-08-4889

this activity profile elicits antitumor effects on both tumor epithelial cells and vasculature. This combination of activities translates into broad and potent inhibition of tumor growth *in vivo*[3] and supports the ongoing clinical evaluation of EXEL-2880.

[3] F.M. Yakes et al., submitted for publication.

Disclosure of Potential Conflicts of Interest

No potential conflicts of interest were disclosed.

Acknowledgments

Received 12/22/08; revised 7/1/09; accepted 8/21/09; published OnlineFirst 10/6/09.

The costs of publication of this article were defrayed in part by the payment of page charges. This article must therefore be hereby marked *advertisement* in accordance with 18 U.S.C. Section 1734 solely to indicate this fact.

References

1. Birchmeier C, Birchmeier W, Gherardi E, Vande Woude GF. Met, metastasis, motility and more. Nat Rev Mol Cell Biol 2003;4:915–25.
2. Huh CG, Factor VM, Sanchez A, Uchida K, Conner EA, Thorgeirsson SS. Hepatocyte growth factor/c-met signaling pathway is required for efficient liver regeneration and repair. Proc Natl Acad Sci U S A 2004;101:4477–82.
3. Comoglio PM, Giordano S, Trusolino L. Drug development of MET inhibitors: targeting oncogene addiction and expedience. Nat Rev Drug Discov 2008;7:504–16.
4. Schmidt L, Duh FM, Chen F, et al. Germline and somatic mutations in the tyrosine kinase domain of the MET proto-oncogene in papillary renal carcinomas. Nat Genet 1997;16:68–73.
5. Takaki Y, Furihata M, Yoshikawa C, Kishida T, Yao M, Shuin T. Sporadic bilateral papillary renal carcinoma exhibiting C-met mutation in the left kidney tumor. J Urol 2000;163:1241–2.
6. Lee JH, Han SU, Cho H, et al. A novel germ line juxtamembrane Met mutation in human gastric cancer. Oncogene 2000;19:4947–53.
7. Park WS, Dong SM, Kim SY, et al. Somatic mutations in the kinase domain of the Met/hepatocyte growth factor receptor gene in childhood hepatocellular carcinomas. Cancer Res 1999;59:307–10.
8. Di Renzo MF, Olivero M, Martone T, et al. Somatic mutations of the MET oncogene are selected during metastatic spread of human HNSC carcinomas. Oncogene 2000;19:1547–55.
9. Tanyi J, Tory K, Rigo J, Jr., Nagy B, Papp Z. Evaluation of the tyrosine kinase domain of the Met proto-oncogene in sporadic ovarian carcinomas*. Pathol Oncol Res 1999;5:187–91.
10. Ma PC, Kijima T, Maulik G, et al. c-MET mutational analysis in small cell lung cancer: novel juxtamembrane domain mutations regulating cytoskeletal functions. Cancer Res 2003;63:6272–81.
11. Bieche I, Champeme MH, Lidereau R. Infrequent mutations of the MET gene in sporadic breast tumours. Int J Cancer 1999;82:908–10.
12. Moon YW, Weil RJ, Pack SD, et al. Missense mutation of the MET gene detected in human glioma. Mod Pathol 2000;13:973–7.
13. Lorenzato A, Olivero M, Patane S, et al. Novel somatic mutations of the MET oncogene in human carcinoma metastases activating cell motility and invasion. Cancer Res 2002;62:7025–30.
14. Zeng ZS, Weiser MR, Kuntz E, et al. c-Met gene amplification is associated with advanced stage colorectal cancer and liver metastases. Cancer Lett 2008;265:258–69.
15. Seruca R, Suijkerbuijk RF, Gartner F, et al. Increasing levels of MYC and MET co-amplification during tumor progression of a case of gastric cancer. Cancer Genet Cytogenet 1995;82:140–5.
16. Kuniyasu H, Yasui W, Kitadai Y, Yokozaki H, Ito H, Tahara E. Frequent amplification of the c-met gene in scirrhous type stomach cancer. Biochem Biophys Res Commun 1992;189:227–32.
17. Umeki K, Shiota G, Kawasaki H. Clinical significance of c-met oncogene alterations in human colorectal cancer. Oncology 1999;56:314–21.
18. Bean J, Brennan C, Shih JY, et al. MET amplification occurs with or without T790M mutations in EGFR mutant lung tumors with acquired resistance to gefitinib or erlotinib. Proc Natl Acad Sci U S A 2007;104:20932–7.
19. Engelman JA, Zejnullahu K, Mitsudomi T, et al. MET amplification leads to gefitinib resistance in lung cancer by activating ERBB3 signaling. Science 2007;316:1039–43.
20. Kawano R, Ohshima K, Karube K, et al. Prognostic significance of hepatocyte growth factor and c-MET expression in patients with diffuse large B-cell lymphoma. Br J Haematol 2004;127:305–7.
21. Lengyel E, Prechtel D, Resau JH, et al. c-Met overexpression in node-positive breast cancer identifies patients with poor clinical outcome independent of Her2/neu. Int J Cancer 2005;113:678–82.
22. Nakajima M, Sawada H, Yamada Y, et al. The prognostic significance of amplification and overexpression of c-met and c-erbB-2 in human gastric carcinomas. Cancer 1999;85:1894–902.
23. Wu F, Wu L, Zheng S, et al. The clinical value of hepatocyte growth factor and its receptor-c-met for liver cancer patients with hepatectomy. Dig Liver Dis 2006;38:490–7.
24. Baykal C, Ayhan A, Al A, Yuce K, Ayhan A. Overexpression of the c-Met/HGF receptor and its prognostic significance in uterine cervix carcinomas. Gynecol Oncol 2003;88:123–9.
25. Bellusci S, Moens G, Gaudino G, et al. Creation of an hepatocyte growth factor/scatter factor autocrine loop in carcinoma cells induces invasive properties associated with increased tumorigenicity. Oncogene 1994;9:1091–9.
26. Rong S, Segal S, Anver M, Resau JH, Vande Woude GF. Invasiveness and metastasis of NIH 3T3 cells induced by Met-hepatocyte growth factor/scatter factor autocrine stimulation. Proc Natl Acad Sci U S A 1994;91:4731–5.
27. Takayama H, LaRochelle WJ, Sharp R, et al. Diverse tumorigenesis associated with aberrant development in mice overexpressing hepatocyte growth factor/scatter factor. Proc Natl Acad Sci U S A 1997;94:701–6.
28. Boccaccio C, Sabatino G, Medico E, et al. The MET oncogene drives a genetic programme linking cancer to haemostasis. Nature 2005;434:396–400.
29. Abounader R, Lal B, Luddy C, et al. *In vivo* targeting of SF/HGF and c-met expression via U1snRNA/ribozymes inhibits glioma growth and angiogenesis and promotes apoptosis. FASEB J 2002;16:108–10.
30. Kim SJ, Johnson M, Koterba K, Herynk MH, Uehara H, Gallick GE. Reduced c-Met expression by an adenovirus expressing a c-Met ribozyme inhibits tumorigenic growth and lymph node metastases of PC3-4 prostate tumor cells in an orthotopic nude mouse model. Clin Cancer Res 2003;9:5161–70.
31. Stabile LP, Lyker JS, Huang L, Siegfried JM. Inhibition of human non-small cell lung tumors by a c-Met antisense/U6 expression plasmid strategy. Gene Ther 2004;11:325–35.
32. Cao B, Su Y, Oskarsson M, et al. Neutralizing monoclonal antibodies to hepatocyte growth factor/scatter factor (HGF/SF) display antitumor activity in animal models. Proc Natl Acad Sci U S A 2001;98:7443–8.
33. Burgess T, Coxon A, Meyer S, et al. Fully human monoclonal antibodies to hepatocyte growth factor with therapeutic potential against hepatocyte growth factor/c-Met-dependent human tumors. Cancer Res 2006;66:1721–9.
34. Martens T, Schmidt NO, Eckerich C, et al. A novel one-armed anti-c-Met antibody inhibits glioblastoma growth *in vivo*. Clin Cancer Res 2006;12:6144–52.
35. Tomioka D, Maehara N, Kuba K, et al. Inhibition of growth, invasion, and metastasis of human pancreatic carcinoma cells by NK4 in an orthotopic mouse model. Cancer Res 2001;61:7518–24.
36. Ferrara N, Gerber HP, LeCouter J. The biology of VEGF and its receptors. Nat Med 2003;9:669–76.
37. Laird AD, Cherrington JM. Small molecule tyrosine kinase inhibitors: clinical development of anticancer agents. Expert Opin Investig Drugs 2003;12:51–64.
38. Pennacchietti S, Michieli P, Galluzzo M, Mazzone M, Giordano S, Comoglio PM. Hypoxia promotes invasive growth by transcriptional activation of the met protooncogene. Cancer Cell 2003;3:347–61.
39. Bottaro DP, Liotta LA. Cancer: out of air is not out of action. Nature 2003;423:593–5.
40. Xin X, Yang S, Ingle G, et al. Hepatocyte growth factor enhances vascular endothelial growth factor-induced angiogenesis *in vitro* and *in vivo*. Am J Pathol 2001;158:1111–20.
41. Bannen LC, Chan DS, Chen J, et al., inventors; c-Met modulators and methods of use. U.S. Patent US WO2005030140.
42. Sepp-Lorenzino L, Rands E, Mao X, et al. A novel orally bioavailable inhibitor of kinase insert domain-containing receptor induces antiangiogenic effects and prevents tumor growth *in vivo*. Cancer Res 2004;64:751–6.
43. Johnson LN, Noble ME, Owen DJ. Active and inactive protein kinases: structural basis for regulation. Cell 1996;85:149–58.
44. Fidler IJ. Biological behavior of malignant melanoma cells correlated to their survival *in vivo*. Cancer Res 1975;35:218–24.
45. Bergers G, Song S, Meyer-Morse N, Bergsland E, Hanahan D. Benefits of targeting both pericytes and endothelial cells in the tumor vasculature with kinase inhibitors. J Clin Invest 2003;111:1287–95.
46. Bellon SF, Kaplan-Lefko P, Yang Y, et al. c-Met inhibitors with novel binding mode show activity against several hereditary papillary renal cell carcinoma-related mutations. J Biol Chem 2008;283:2675–83.
47. Cai ZW, Wei D, Schroeder GM, et al. Discovery of orally active pyrrolopyridine- and aminopyridine-based Met kinase inhibitors. Bioorg Med Chem Lett 2008;18:3224–9.
48. Schiering N, Knapp S, Marconi M, et al. Crystal structure of the tyrosine kinase domain of the hepatocyte growth factor receptor c-Met and its complex with the microbial alkaloid K-252a. Proc Natl Acad Sci U S A 2003;100:12654–9.
49. Wang W, Marimuthu A, Tsai J, et al. Structural characterization of autoinhibited c-Met kinase produced by coexpression in bacteria with phosphatase. Proc Natl Acad Sci U S A 2006;103:3563–8.

Cancer Research
The Journal of Cancer Research (1916–1930) | The American Journal of Cancer (1931–1940)

AACR American Association for Cancer Research

Inhibition of Tumor Cell Growth, Invasion, and Metastasis by EXEL-2880 (XL880, GSK1363089), a Novel Inhibitor of HGF and VEGF Receptor Tyrosine Kinases

Fawn Qian, Stefan Engst, Kyoko Yamaguchi, et al.

Cancer Res 2009;69:8009-8016. Published OnlineFirst October 6, 2009.